

INTERPRETING POWER ANISOTROPY MEASUREMENTS IN PLASMA TURBULENCE

C. H. K. CHEN¹, R. T. WICKS¹, T. S. HORBURY¹, AND A. A. SCHEKOCIHIN²

¹The Blackett Laboratory, Imperial College London, London SW7 2AZ, UK; christopher.chen03@imperial.ac.uk

²Rudolf Peierls Centre for Theoretical Physics, University of Oxford, Oxford OX1 3NP, UK

Submitted 2009 September 14; accepted 2010 January 27; published 2010 February 19

ABSTRACT

A relationship is derived between power anisotropy and wavevector anisotropy in turbulent fluctuations. This can be used to interpret plasma turbulence measurements, for example, in the solar wind. If fluctuations are spatially anisotropic, then the ion gyroscale break point in measured spectra in the directions parallel and perpendicular to the magnetic field would not occur at the same frequency, and similarly for the electron gyroscale break point. This is an important consideration when interpreting solar wind measurements in terms of anisotropic turbulence theories. Model magnetic field power spectra are presented assuming a cascade of critically balanced Alfvén waves in the inertial range and kinetic Alfvén waves in the dissipation range. The variation of power anisotropy with scale is compared to existing solar wind measurements, and the similarities and differences are discussed.

Subject headings: magnetic fields – magnetohydrodynamics (MHD) – plasmas – solar wind – turbulence

1. INTRODUCTION

Plasma turbulence is observed to be anisotropic with respect to the magnetic field direction. For example, in the solar wind, the observed power and scaling of turbulent fluctuations vary depending on the angle between the local mean field and the sampling direction (Bieber et al. 1996; Horbury et al. 2008; Podesta 2009; Osman & Horbury 2009). Correlation functions have also been observed to be anisotropic in the solar wind (Crooker et al. 1982; Matthaeus et al. 1990; Osman & Horbury 2007; Weygand et al. 2009) and laboratory measurements (Robinson & Rusbridge 1971; Zweben et al. 1979).

Recent theories of plasma turbulence assume anisotropy (Goldreich & Sridhar 1995; Boldyrev 2006; Galtier 2006; Lithwick et al. 2007; Gogoberidze 2007; Chandran 2008; Beresnyak & Lazarian 2008; Podesta & Bhattacharjee 2009; Schekochihin et al. 2009) and anisotropic energy transfer has been seen in simulations (Shebalin et al. 1983; Cho & Vishniac 2000; Maron & Goldreich 2001; Cho et al. 2002; Cho & Lazarian 2004, 2009). The theories usually describe the anisotropy in terms of the fluctuation wavenumbers parallel and perpendicular to the mean magnetic field direction, k_{\parallel} and k_{\perp} . For example, Goldreich & Sridhar (1995) used the “critical balance” assumption to obtain $k_{\parallel} \sim k_{\perp}^{2/3}$ for magnetohydrodynamic (MHD) turbulence and, more generally, theories often assume $k_{\perp} \gg k_{\parallel}$. In the solar wind, however, it is the anisotropy in power at a fixed scale that is often measured for practical reasons, rather than the spatial anisotropy of the fluctuations.

In Section 2, the relationship between power anisotropy and wavevector anisotropy is derived. A critically balanced model is then presented in Section 3 to illustrate that a break point in an anisotropic spectrum may occur at different scales when the reduced spectrum is observed in different directions. The implications of these two sections for recent solar wind measurements are discussed in Section 4.

2. POWER ANISOTROPY AND WAVEVECTOR ANISOTROPY

The correlation function of a turbulent field, for example, the magnetic field, \mathbf{B} , can be defined as $C(\mathbf{x}) = \langle \mathbf{B}(\mathbf{r} + \mathbf{x}) \cdot \mathbf{B}(\mathbf{r}) \rangle$, where the angular brackets denote an ensemble average over positions \mathbf{r} . The three-dimensional energy spectrum can then be defined as the Fourier transform of the correlation function, $E(\mathbf{k}) = \int C(\mathbf{k}) e^{-i\mathbf{k} \cdot \mathbf{x}} d^3\mathbf{x}$.

A single spacecraft in the solar wind measures the turbulent field as a function of time, $\mathbf{B}(t)$. Since the solar wind velocity, \mathbf{v}_{sw} , is much larger than the wave speed (often taken as the Alfvén speed in the inertial range), Taylor’s hypothesis (Taylor 1938) is usually well satisfied, meaning that the measured time variations correspond to spatial fluctuations in the plasma, $\Delta\mathbf{x} = -\mathbf{v}_{\text{sw}}\Delta t$. Because a single spacecraft gives a one-dimensional cut through the plasma, the full three-dimensional spectrum cannot be measured but instead a reduced version is obtained (Fredricks & Coroniti 1976). This reduced spectrum, defined as $P(k) = \int E(\mathbf{k}') \delta(k - \mathbf{k}' \cdot \hat{\mathbf{v}}_{\text{sw}}) d^3\mathbf{k}'$, where $\hat{\mathbf{v}}_{\text{sw}}$ is the solar wind direction unit vector, is the three-dimensional spectrum integrated over the directions perpendicular to the measuring direction. Assuming axisymmetry about the magnetic field, this reduced power spectrum also depends on the angle, θ , of the field to the one-dimensional measurement direction, $P(k, \theta)$. In Cartesian coordinates, this can be written as a dependence on the parallel and perpendicular wavenumbers, $P(k_{\parallel}, k_{\perp})$.

Figure 1 is a schematic of reduced power contours with respect to the parallel and perpendicular wavenumbers. Power anisotropy is usually measured at a fixed scale, indicated by the red dashed line which is at a fixed radius from the origin. At different points along this line, a different reduced power is sampled; this effect is readily seen in the solar wind (Bieber et al. 1996; Horbury et al. 2008; Podesta 2009; Osman & Horbury 2009). A relationship between power anisotropy and wavevector anisotropy will now be derived. Note that the derivation does not depend on any particular contour shape; the elliptical shapes in the figure are for illus-

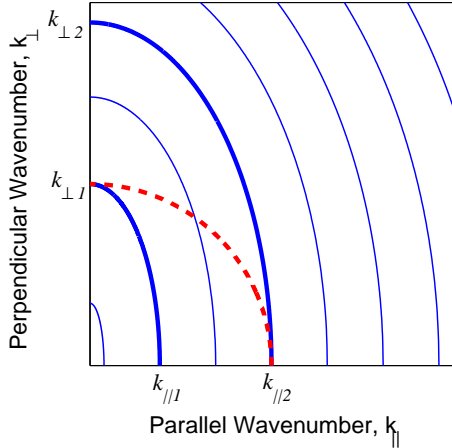


Figure 1. Schematic of reduced power contours (solid blue lines) elongated in the field parallel direction. Power anisotropy measurements are made at a fixed scale (dashed red line).

trative purposes only.

Let us consider two contours of size $(k_{\parallel 1}, k_{\perp 1})$ and $(k_{\parallel 2}, k_{\perp 2})$ such that $k_{\parallel 2} = k_{\perp 1}$ (Figure 1). We will assume that power anisotropy is being measured at this wavenumber, $k = k_{\parallel 2} = k_{\perp 1}$. Let reduced power in the parallel and perpendicular directions be defined as $P_{\parallel} = P(k_{\parallel}, 0)$ and $P_{\perp} = P(0, k_{\perp})$, and α be the scaling exponent in the perpendicular direction, $P_{\perp} \sim k_{\perp}^{-\alpha}$. Dividing the equations for P_{\perp} for each contour we get

$$\frac{P_{\perp 1}}{P_{\perp 2}} = \left(\frac{k_{\perp 2}}{k_{\perp 1}} \right)^{\alpha}. \quad (1)$$

By the definition of a contour, $P_{\perp 2} = P_{\parallel 2}$ and from the above definition of the two contours, $k_{\parallel 2} = k_{\perp 1}$. Substituting these into Equation (1) gives

$$\frac{P_{\perp 1}}{P_{\parallel 2}} = \left(\frac{k_{\perp 2}}{k_{\parallel 2}} \right)^{\alpha}. \quad (2)$$

Since $P_{\perp 1}/P_{\parallel 2}$ is just the power anisotropy at fixed wavenumber k (as in solar wind measurements), the numeric subscripts may be dropped. Rearranging Equation (2) we get

$$\left(\frac{k_{\perp}}{k_{\parallel}} \right)_2 = \left(\frac{P_{\perp}}{P_{\parallel}} \right)^{\frac{1}{\alpha}}. \quad (3)$$

This relationship is independent of the scaling of the parallel spectrum and allows us to calculate the wavevector anisotropy of contour 2 from a measurement of P_{\perp}/P_{\parallel} . A similar relationship can be derived for contour 1,

$$\left(\frac{k_{\perp}}{k_{\parallel}} \right)_1 = \left(\frac{P_{\perp}}{P_{\parallel}} \right)^{\frac{1}{\beta}}, \quad (4)$$

where β is the scaling exponent of the parallel reduced spectrum, $P_{\parallel} \sim k_{\parallel}^{-\beta}$. Although it is possible to infer the wavevector anisotropy from the interpolation of measurements such as Figure 1 of Horbury et al. (2008), the relationship given here allows it to be found from the power anisotropy, a quantity more easily measurable in the solar wind.

The k_{\perp} and k_{\parallel} of turbulence theories usually describe typical length scales associated with the fluctuations. It is usu-

ally assumed that second-order statistics, such as power, relate to these quantities, for example Cho & Vishniac (2000) state that in their simulations, contours of second-order structure functions “reflect the shapes of the eddies.” Under this assumption, the wavevector anisotropy of power contours can be thought to describe “typical” wavevector anisotropy of the fluctuations.

3. FORM OF THE CRITICAL BALANCE REDUCED POWER SPECTRUM

The “critical balance” assumption states that in a turbulent Alfvén wave (AW) cascade, the linear wave timescale and the nonlinear energy transfer timescale are comparable. It was introduced explicitly by Goldreich & Sridhar (1995) and anticipated in the work of Higdon (1984). When applied to inertial range MHD turbulence, the spectral index of the reduced spectrum in the perpendicular direction is $-5/3$ and the wavevector scaling is $k_{\parallel} \sim k_{\perp}^{2/3}$. A reduced spectral index of -2 in the parallel direction follows from these statements.

There is evidence in the solar wind inertial range for both the Alfvénic nature of the turbulence (e.g. Belcher & Davis 1971; Horbury et al. 1995; Bale et al. 2005) and the anisotropic scaling (Horbury et al. 2008). It appears that this scaling is only detectable when observing with respect to the scale-dependent *local* mean magnetic field (e.g. Cho & Vishniac 2000; Horbury et al. 2008; Beresnyak & Lazarian 2009), i.e., the mean field at the scale of each fluctuation being measured, rather than a global large-scale average field. Although MHD is a fluid theory, Schekochihin et al. (2009) have shown that reduced MHD, an anisotropic limit of MHD containing the Alfvénic fluctuations, can be derived for a collisionless plasma at scales larger than the ion gyroradius. This may explain why the MHD scalings are seen in the collisionless solar wind.

At scales smaller than the ion gyroradius, commonly termed the “dissipation range,” there is evidence for kinetic Alfvén waves (KAWs) (Bale et al. 2005; Sahraoui et al. 2009). These are linear modes of electron reduced MHD, an anisotropic theory derived for collisionless plasmas at scales between the electron and ion gyroradii (Schekochihin et al. 2009). When the critical balance assumption is applied to a KAW cascade, the wavevector scaling becomes $k_{\parallel} \sim k_{\perp}^{1/3}$ and the predicted spectral indices for the magnetic field are $-7/3$ in the perpendicular direction and -5 in the parallel direction (Cho & Lazarian 2004; Schekochihin et al. 2009).

In this theoretical framework, the break between the inertial range and the dissipation range is predicted to be at $k_{\perp} \rho_i \sim 1$, where ρ_i is the ion gyroradius, but if the fluctuations here are anisotropic then their parallel length should be larger, $k_{\parallel} \rho_i < 1$. This would imply that the observed break points in solar wind measurements are at different spacecraft frequencies for the reduced spectra in the parallel and perpendicular directions. A similar effect would be expected at the electron break scale, $k_{\perp} \rho_e \sim 1$, where the difference in break frequency between the spectra in the parallel and perpendicular directions may be even greater if the anisotropy continues to increase throughout the dissipation range.

Since the observed break points would be at different scales for spectra in the parallel and perpendicular directions, a schematic of the reduced spectra can be divided into five ranges (Figure 2). In range 1 both spectra display AW scaling; in range 2 the spectrum in the parallel direction has KAW scaling and the spectrum in the perpendicular direction has

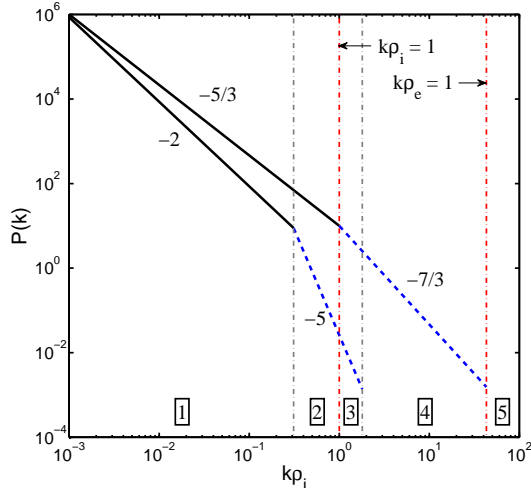


Figure 2. Schematic of magnetic field reduced power spectra in the parallel and perpendicular directions for critically balanced AW (solid black lines) and KAW (dashed blue lines) turbulence.

Table 1
Power Scaling Exponent Predictions for Critically
Balanced AW and KAW Turbulence

Range	P_{\perp} Scaling	P_{\parallel} Scaling	P_{\perp}/P_{\parallel} Scaling
1	-5/3	-2	1/3
2	-5/3	-5	10/3
3	-7/3	-5	8/3
4	-7/3
5

AW scaling; in range 3 both spectra display KAW scaling; in range 4 the spectrum in the parallel direction is below the electron break scale and the spectrum in the perpendicular direction has KAW scaling; in range 5 both spectra are below the electron break scale. Predictions for fluctuations smaller than the electron scale do exist but have not been included here. Gyrokinetic theory predicts scalings for an electron-entropy cascade, valid for $k_{\perp}\rho_e \gg 1$ (Schekochihin et al. 2009), however it has been suggested that it is not applicable to the solar wind in this range (Howes et al. 2008). In Figure 2, the (logarithm of the) power anisotropy can be thought of as the vertical distance between the spectra and the (logarithm of the) wavevector anisotropy as the horizontal distance.

The scalings for each of the ranges in Figure 2 are given in Table 1. Also listed is the scaling of P_{\perp}/P_{\parallel} , which follows directly from that of P_{\perp} and P_{\parallel} and is shown in Figure 3. In the inertial range P_{\perp}/P_{\parallel} scales as $k^{1/3}$ which steepens to $k^{10/3}$ when P_{\parallel} reaches the ion break scale and then becomes shallower at $k^{8/3}$ when P_{\perp} reaches the ion break scale.

The width of the KAW range in the P_{\perp} spectrum is predicted to be $\rho_i/\rho_e = \sqrt{T_i m_i/T_e m_e}$, where m_i and m_e are the ion and electron masses, and for the model spectra in Figures 2 and 3 the temperatures have been assumed equal, $T_i = T_e$. Although T_i/T_e is of order unity in the solar wind, there is some variation (Bruno & Carbone 2005) so the extent of the possible KAW range may vary. The width of each of the ranges in Figures 2 and 3 also depends on the amount of anisotropy present. For example, as the anisotropy at the ion break scale increases, the size of range 2 increases but the size of range

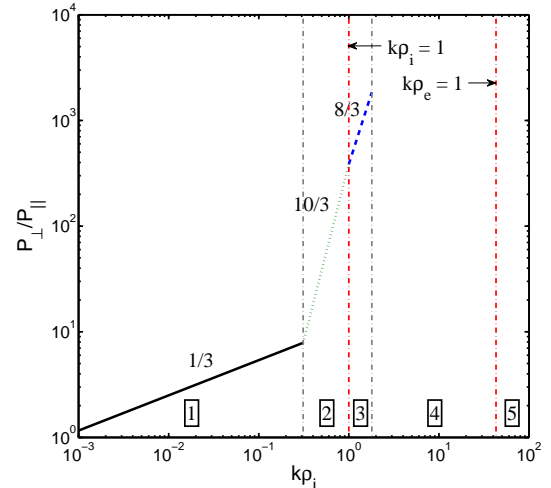


Figure 3. Schematic of reduced power anisotropy as a function of scale for critically balanced AW and KAW turbulence.

3 decreases. It may even be the case that if the anisotropy is very strong at the ion break scale then range 3 may not be present at all, meaning it would not be possible to measure KAW scaling in P_{\perp} and P_{\parallel} at the same frequency.

One of the assumptions used when constructing these model spectra was that they contain no additional energy injection or loss. As noted in Schekochihin et al. (2009), at the ion break scale some energy may be transferred from the Alfvénic cascade channel to a purely electrostatic “entropy cascade.” The amount of energy transferred, if any, is unknown so cannot be included in our model spectra here. It is also possible that power may be injected into the cascades from other sources such as plasma instabilities, for example, the firehose and mirror instabilities, which evidence suggests may be important in the solar wind (Bale et al. 2009). Including effects such as these in this model is beyond the scope of this Letter.

It should also be noted that only the Alfvénic part of the cascade in the inertial range is dealt with here. This is relevant to the solar wind, which is primarily Alfvénic in nature (e.g. Belcher & Davis 1971; Bale et al. 2005; Bruno & Carbone 2005) and in which any compressive (non-Alfvénic) fluctuations are, on theoretical grounds, not thought to interfere with the Alfvénic cascade (Cho & Lazarian 2003; Schekochihin et al. 2009).

4. COMPARISON TO SOLAR WIND MEASUREMENTS

The only published measurement of the variation of power anisotropy, P_{\perp}/P_{\parallel} , in the solar wind across both inertial and dissipation ranges, which we are aware of, is in the lower panel of Figure 7 of Podesta (2009). The scaling arguments in Section 2 can be applied to these measurements to obtain estimates of the wavevector anisotropy at various scales. For example, at the high-frequency end of the inertial range, at ≈ 0.2 Hz, $P_{\perp}/P_{\parallel} \approx 7$ which, using $\alpha = 5/3$ in Equation (3), means $k_{\perp}/k_{\parallel} \approx 3$. A value of $\alpha = 5/3$ was used for this calculation since it is the prediction of critical balance MHD turbulence (Goldreich & Sridhar 1995) and is close to the measured value of 1.65 for this data interval (Podesta 2009). In general, break points in spectra seem to have a rollover rather than a clean break in scaling so this result is approximate. It is also possible that since P_{\parallel} is measured in the bin $0 - 6^{\circ}$ and

not at exactly 0° , values of P_\perp/P_\parallel and therefore k_\perp/k_\parallel may be underestimates. The value obtained here, $k_\perp/k_\parallel \approx 3$, was used to set the anisotropy at the ion break scale in Figures 2 and 3.

Figure 3 of this Letter can be compared to Figure 7 of Podesta (2009) in which the frequency corresponding to $k\rho_i = 1$ is ≈ 0.5 Hz. In the inertial range, both graphs have a shallow slope with the measurement steeper than the prediction, although the uncertainties in the measured slope may be significant as discussed in Podesta (2009). Between 0.4 Hz and 1.0 Hz, the measured power anisotropy increases with a steep slope. The scales at which this happens approximately correspond to ranges 2 and 3 in Figure 3. It may be the case, therefore, that the steep slope of P_\perp/P_\parallel seen in dissipation range solar wind measurements is due to critical balance scaling, in particular the steep scaling of the KAW P_\parallel spectrum.

One difference between the figures is that the decrease in power anisotropy between 0.2 Hz and 0.4 Hz in the measurement is not present in Figure 3. As discussed in Podesta (2009), this is caused by an increase in the parallel power and may be due to parallel waves, for example, from plasma instabilities. For frequencies above 1.0 Hz the measured anisotropy decreases, which is due to the flattening of the P_\parallel spectrum. The scale at which this begins (1.0 Hz) is close to the predicted electron break scale for the P_\parallel spectrum, although without knowing the electron gyroradius, the exact location of this is not clear. One possibility, therefore, is that the cause of this decrease in P_\perp/P_\parallel may be due to the P_\parallel spectrum flattening above the electron break scale. Another possibility is that the cyclotron resonance may have been reached here, causing a change in behavior (Howes et al. 2008). At these high frequencies, however, measurement effects, such as magnetometer noise, may be important and one must be cautious when drawing any conclusions from this range.

Extrapolating the model spectra to larger scales, it can be seen from Figures 2 and 3 that power (and wavevector) isotropy is reached at $k\rho_i \approx 10^{-3}$. This corresponds to a length around 10^6 km or an observed spacecraft frequency of 5×10^{-4} Hz. This is close to the observed break between the low-frequency f^{-1} power law and the inertial range (e.g. Bavassano et al. 1982; Bruno & Carbone 2005) and also the solar wind correlation length (e.g. Matthaeus & Goldstein 1982), scales usually associated with the outer scale of the turbulence.

The solar wind spectrum has recently been observed at scales near $k\rho_e = 1$. Alexandrova et al. (2009) suggest that just above this scale there is an exponential falloff in the spectrum, and Sahraoui et al. (2009) suggest that below it, there is a further steeper power law. Both of these studies involved solar wind intervals where the magnetic field was not aligned with the solar wind direction so that one would expect to see the spectrum in the perpendicular direction. Sahraoui et al. (2009) also plot the spectrum of the parallel component of the magnetic field, which, it should be pointed out for clarity, is not the same as the spectrum in the parallel direction.

5. SUMMARY AND CONCLUSIONS

In Section 2, a relationship was derived that allows the turbulent wavevector anisotropy, k_\perp/k_\parallel , to be inferred from power anisotropy measurements, P_\perp/P_\parallel . This is independent of any particular turbulence theory and only assumes power-law scaling in the parallel and perpendicular directions. Using this relation and existing solar wind measurements (Podesta

2009) the wavevector anisotropy near the ion break scale was estimated to be $k_\perp/k_\parallel \approx 3$, although this may be an underestimate due to the finite angular resolution of the measurements.

Model spectra of critically balanced AWs (for the inertial range) and KAWs (for the dissipation range) were presented to illustrate that break points do not occur at the same scale in the observed spectra in the parallel and perpendicular directions if the turbulence is anisotropic. The variation of P_\perp/P_\parallel with scale was calculated from these model spectra resulting in five ranges, three of which have predictions of how P_\perp/P_\parallel scales: a $1/3$ range, a $10/3$ range, and an $8/3$ range. If the wavevector anisotropy is significant then some of these ranges are small and may not even be present. Some of these features can be seen in the measurements of Podesta (2009). The main difference is the extra parallel power at the ion break scale seen in the measurements, which may be due to energy injection mechanisms at the ion gyroscale.

Although critically balanced AWs and KAWs were used in Section 3, the ideas also apply to anisotropic theories of plasma turbulence in general. Some of these, for example, are a nonlocal cascade model (Gogoberidze 2007), turbulence with dynamic alignment (Boldyrev 2006; Podesta & Bhattacharjee 2009), wave turbulence in Hall MHD (Galtier 2006), and imbalanced turbulence (Lithwick et al. 2007; Beresnyak & Lazarian 2008; Chandran 2008). The anisotropy relationship derived in Section 2 and the observational considerations discussed in Sections 3 and 4 are also applicable to these theories and any possible extensions of them into the dissipation range.

This work was funded by STFC and the Leverhulme Trust International Academic Network for Magnetized Plasma Turbulence. C. Chen acknowledges helpful discussions with T. Yousef and A. Mallet and useful comments from an anonymous referee.

REFERENCES

- Alexandrova, O., Saur, J., Lacombe, C., Mangeney, A., Mitchell, J., Schwartz, S. J., & Robert, P. 2009, *Phys. Rev. Lett.*, 103, 165003
 Bale, S. D., Kasper, J. C., Howes, G. G., Quataert, E., Salem, C., & Sundkvist, D. 2009, *Phys. Rev. Lett.*, 103, 211101
 Bale, S. D., Kellogg, P. J., Mozer, F. S., Horbury, T. S., & Reme, H. 2005, *Phys. Rev. Lett.*, 94, 215002
 Bavassano, B., Dobrowolny, M., Mariani, F., & Ness, N. F. 1982, *J. Geophys. Res.*, 87, 3617
 Belcher, J. W., & Davis, L., Jr. 1971, *J. Geophys. Res.*, 76, 3534
 Beresnyak, A., & Lazarian, A. 2008, *ApJ*, 682, 1070
 —. 2009, *ApJ*, 702, 460
 Bieber, J. W., Wanner, W., & Matthaeus, W. H. 1996, *J. Geophys. Res.*, 101, 2511
 Boldyrev, S. 2006, *Phys. Rev. Lett.*, 96, 115002
 Bruno, R., & Carbone, V. 2005, *Living Rev. Sol. Phys.*, 2, 4
 Chandran, B. D. G. 2008, *ApJ*, 685, 646
 Cho, J., & Lazarian, A. 2003, *MNRAS*, 345, 325
 —. 2004, *ApJ*, 615, L41
 —. 2009, *ApJ*, 701, 236
 Cho, J., Lazarian, A., & Vishniac, E. T. 2002, *ApJ*, 564, 291
 Cho, J., & Vishniac, E. T. 2000, *ApJ*, 539, 273
 Crooker, N. U., Siscoe, G. L., Russell, C. T., & Smith, E. J. 1982, *J. Geophys. Res.*, 87, 2224
 Fredricks, R. W., & Coroniti, F. V. 1976, *J. Geophys. Res.*, 81, 5591
 Galtier, S. 2006, *J. Low Temp. Phys.*, 145, 59
 Gogoberidze, G. 2007, *Phys. Plasmas*, 14, 022304
 Goldreich, P., & Sridhar, S. 1995, *ApJ*, 438, 763
 Higdon, J. C. 1984, *ApJ*, 285, 109
 Horbury, T. S., Balogh, A., Forsyth, R. J., & Smith, E. J. 1995, *Geophys. Res. Lett.*, 22, 3405
 Horbury, T. S., Forman, M., & Oughton, S. 2008, *Phys. Rev. Lett.*, 101, 175005
 Howes, G. G., Cowley, S. C., Dorland, W., Hammett, G. W., Quataert, E., & Schekochihin, A. A. 2008, *J. Geophys. Res.*, 113, 5103
 Lithwick, Y., Goldreich, P., & Sridhar, S. 2007, *ApJ*, 655, 269

- Maron, J., & Goldreich, P. 2001, *ApJ*, 554, 1175
- Matthaeus, W. H., & Goldstein, M. L. 1982, *J. Geophys. Res.*, 87, 6011
- Matthaeus, W. H., Goldstein, M. L., & Roberts, D. A. 1990, *J. Geophys. Res.*, 95, 20673
- Osman, K. T., & Horbury, T. S. 2007, *ApJ*, 654, L103
- . 2009, *Ann. Geophys.*, 27, 3019
- Podesta, J. J. 2009, *ApJ*, 698, 986
- Podesta, J. J., & Bhattacharjee, A. 2009, *Phys. Rev. Lett.*, submitted (arXiv:0903.5041 v1)
- Robinson, D. C., & Rusbridge, M. G. 1971, *Phys. Fluids*, 14, 2499
- Sahraoui, F., Goldstein, M. L., Robert, P., & Khotyaintsev, Y. V. 2009, *Phys. Rev. Lett.*, 102, 231102
- Schekochihin, A. A., Cowley, S. C., Dorland, W., Hammett, G. W., Howes, G. G., Quataert, E., & Tatsuno, T. 2009, *ApJS*, 182, 310
- Shebalin, J. V., Matthaeus, W. H., & Montgomery, D. 1983, *J. Plasma Phys.*, 29, 525
- Taylor, G. I. 1938, *Proc. R. Soc. A*, 164, 476
- Weygand, J. M., Matthaeus, W. H., Dasso, S., Kivelson, M. G., Kistler, L. M., & Mouikis, C. 2009, *J. Geophys. Res.*, 114, 7213
- Zweben, S. J., Menyuk, C. R., & Taylor, R. J. 1979, *Phys. Rev. Lett.*, 42, 1270